

## Evidence for charging effects in CdTe/CdMgTe quantum point contacts

M. Czapkiewicz,\* V. Kolkovsky, P. Nowicki, M. Wiater, T. Wojciechowski, T. Wojtowicz, and J. Wróbel  
*Institute of Physics, Polish Academy of Sciences, al Lotników 32/46, 02-668 Warszawa, Poland*  
 (Received 24 April 2012; revised manuscript received 27 August 2012; published 9 October 2012)

Here we report on fabrication and low-temperature magnetotransport measurements of quantum point contacts patterned from a novel two-dimensional electron system—CdTe/CdMgTe modulation doped heterostructure. From the temperature and bias dependence we ascribe the reported data to evidence for a weakly bound state which is naturally formed inside a CdTe quantum constriction due to charging effects. We argue that the spontaneous introduction of an open dot is responsible for replacement of flat conductance plateaus by quasiperiodic resonances with amplitude less than  $2e^2/h$ , as found in our system. Additionally, below 1 K a pattern of weaker conductance peaks, superimposed upon wider resonances, is also observed.

DOI: [10.1103/PhysRevB.86.165415](https://doi.org/10.1103/PhysRevB.86.165415)

PACS number(s): 73.63.Rt, 73.23.Ad

Quantum point contacts (QPCs) are conventionally considered as open mesoscopic systems and their characteristic feature, i.e., integer quantized conductance  $G$ , is well understood as a single electron effect.<sup>1</sup> Nevertheless, some additional noninteger anomalous resonances are also commonly observed at low temperatures and their exact origin is under active debate. Generally they are attributed to electron-electron ( $e$ - $e$ ) interactions and more specifically, to the formation of quasibound states inside the constriction. Such charge droplets may reveal the Kondo physics or become, via the exchange energy term, ferromagnetically polarized.<sup>2</sup> To date, the physical mechanism of localization is still unclear and the role of charging effects<sup>3</sup> in the spontaneous formation of an open dot remains controversial. Therefore, a semiconducting material with a large ratio of Coulomb to kinetic energies is expedient to resolve these important issues and is potentially useful for spintronic applications.

Motivated by these considerations we report on fabrication and low-temperature magnetotransport measurements of quantum point contacts, patterned from  $n$ -type CdTe/CdMgTe modulation doped quantum well (QW), studied in the ballistic transport regime. It is expected that the correlation effects in CdTe are stronger, as compared to GaAs, since the effective mass is larger and the dielectric constant is smaller. As a result, the average distance between electrons  $r_s$ , expressed in effective Bohr radius units, is 2.2 times larger for CdTe than for GaAs with the same carrier density. In this paper we provide evidence for a spontaneous formation of a quasibound state in short and nominally symmetric QPCs, which suggests that the counterintuitive appearance of localization is caused by  $e$ - $e$  correlations. This is supported by the temperature and bias dependence of observed conductance resonances.

The 15-nm-wide CdTe quantum well, modulation doped on one side with iodine, and embedded between Cd<sub>1-y</sub>Mg<sub>y</sub>Te barriers has been used to produce QPCs. The structure was grown by molecular beam epitaxy (MBE) on a commercial epitaxially (100)-GaAs substrate oriented 2° off towards  $\langle 110 \rangle$ . Prior to the growth of actual quantum structure on the strongly lattice mismatched GaAs the proper buffer layers were deposited. The QW itself was grown with the use of regular MBE growth mode but with the first and the last six monolayers grown by ALE (atomic layer epitaxy, i.e. alternating supply of Cd and Te fluxes). Iodine donors were introduced remotely into

the 5-nm-thick Cd<sub>1-y</sub>Mg<sub>y</sub>Te part of the barrier at a distance of 15 nm from the QW in the growth direction. Finally a 50-nm-thick undoped CdMgTe cap concluded the structure. Growth rates were determined from the reflection high-energy electron diffraction (RHEED) intensity oscillations and the concentration of Mg in the barrier was found from the position of the barrier related photoluminescence peak to be  $y = 0.28$ . The density of two-dimensional electron gas (2DEG)  $n_{2D}$  and its mobility  $\mu$  were determined from Hall and conductivity measurements performed on six probes of a Hall bar sample to be  $5.6 \times 10^{11} \text{ cm}^{-2}$  and  $2.3 \times 10^5 \text{ cm}^2/\text{V s}$ , respectively. In Fig. 1 we plot the magnetoresistivity tensor components obtained for a quantum well which has been cooled down in the dark.

On such structure the four-terminal quantum point contacts of length  $L \approx 200 \text{ nm}$  and lithographic width  $W_{\text{lith}} = 450 \pm 10 \text{ nm}$  have been patterned by  $e$ -beam lithography and deep-etching techniques. Carrier density in those devices is controlled by means of V-shaped *side gates* which are separated from the constriction area by narrow etched grooves (see inset to Fig. 2) and macroscopic electrical contacts have been prepared by direct indium soldering. The differential conductance  $G$  has been measured in a He-3 cryostat as a function of dc source-drain bias and *in-plane* magnetic field by employing a standard low-frequency lock-in technique, with ac excitation voltage of 50  $\mu\text{V}$ .

The four-terminal method of measurements is essential for transport studies of CdTe based materials since the indium contacts often show a nonlinear (but symmetric)  $I$ - $V$  characteristics. We have observed the zero-bias contact resistances  $R_k \approx 60 \text{ k}\Omega$  and this value drops to about 5  $\text{k}\Omega$  for  $V_{\text{SD}}^* \gtrsim 1 \text{ mV}$ , where  $V_{\text{SD}}^*$  is the dc source-drain voltage applied to the device. Since indium has been annealed far away (few mm) from the QPC region, contact resistances do not depend on gate voltage  $V_g$ . However, a weak increase with temperature (15% from 0.3 to 2 K) and magnetic field (25% from 0 to 5 T) has been observed.  $R_k$  has not varied upon a thermal cycling and conductance data collected at different cooldowns to  $T = 0.3 \text{ K}$  demonstrate similar characteristics.

We have studied several devices of the same geometry, however, perfect conductance quantization with  $G_0 = 2e^2/h$  plateaus has *never* been observed. The electron mean free path of the 2DEG is  $\ell \approx 3 \mu\text{m}$  and chemically etched grooves

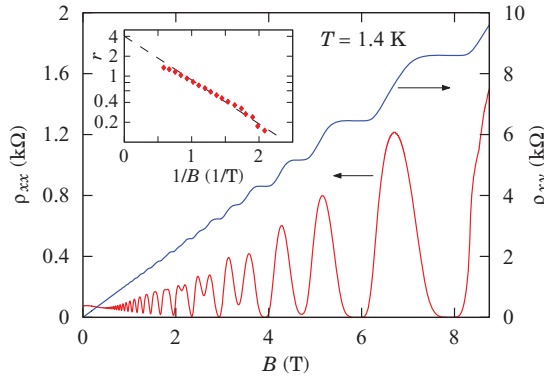


FIG. 1. (Color online) Longitudinal  $\rho_{xx}$  and Hall  $\rho_{xy}$  resistances versus perpendicular magnetic field  $B$  for two-dimensional electron gas in CdTe/CdMgTe quantum well (at temperature 1.4 K). Inset shows a Dingle plot of the reduced SdH oscillations amplitude  $r = \Delta\rho_{xx}/\mathcal{X}\rho_0$ , where  $\rho_0 = \rho_{xx}(0)$  and  $\mathcal{X}$  is the function of temperature and inverse magnetic field, defined in Ref. 4.

are rather smooth. Also, the estimated physical width of the constriction  $W$  is much smaller than  $W_{\text{lith}}$  (see below) so the influence of side-wall roughness is reduced. To determine the dominant scattering mechanism in CdTe quantum wells we have estimated the single-particle relaxation time (also known as the quantum lifetime)  $\tau_q = 1.2 \pm 0.1$  ps from the Shubnikov–de Haas (SdH) oscillations data shown in Fig. 1, using the standard procedure.<sup>4</sup> It is expected that for the short-range background impurity scattering  $\tau_q$  is equivalent to the transport relaxation time  $\tau_t$ , obtained from the mobility. In our case, however,  $\tau_t$  is approximately 12 times longer than  $\tau_q$  and an even larger value of  $\tau_t/\tau_q$  parameter has been recently reported for similar 20 nm CdTe QW.<sup>5</sup> According to Ref. 6,  $\tau_t/\tau_q \gtrsim 10$  implies that 2DEG electrons in GaAs scatter predominantly on smooth potential fluctuations, which originate from the remote impurities. Consequently, the same momentum relaxation mechanism, without strong

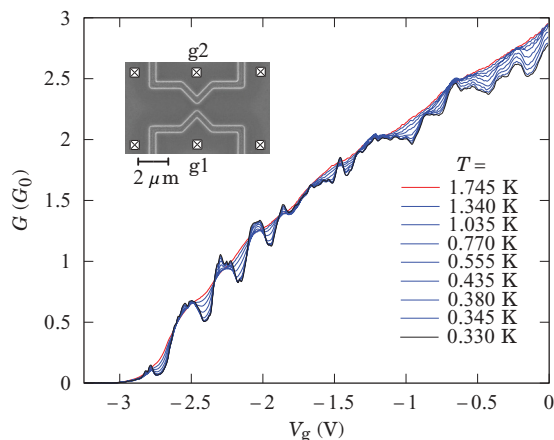


FIG. 2. (Color online) The zero-bias differential conductance  $G = dI/dV$  (in  $G_0 = 2e^2/h$  units) as a function of gate voltage  $V_g$  for temperatures  $T$  from 0.330 to 1.745 K. The inset displays an electron micrograph of a typical device, electrical contacts are shown schematically, side gates are marked with  $g_1$  and  $g_2$ .  $V_g$  have been applied symmetrically, i.e.,  $V_g = V_{g_1} = V_{g_2}$ .

backscattering, is also expected in our samples. For GaAs heterostructures, a comparable value of  $\tau_t/\tau_q$  ratio corresponds to carrier mobilities  $\mu > 5.0 \times 10^5$  cm<sup>2</sup>/Vs (see Ref. 4), therefore the absence of flat conductance steps in CdTe point contacts is quite unexpected.

Figure 2 shows differential conductance data, obtained for the most comprehensively studied QPC sample.  $G$  is not perfectly quantized vs gate voltage, however, quasiperiodic conductance oscillations with amplitude less than  $G_0$  are clearly visible. Additionally, at low temperatures ( $T < 1.4$  K) a weaker pattern of less regular and narrower fluctuations is observed. Some of the random fluctuations are caused by disorder, but regular conductance resonances with amplitude reduced down to  $\approx 0.6 \times (2e^2/h)$  must be related to a subsequent population of one-dimensional (1D) channels.

Reduced steps and conductance resonances had been already observed for longer quantum wires or disordered QPCs made of AlGaAs/GaAs heterostructures.<sup>1,7</sup> They are commonly attributed to a single electron interference and backscattering effects caused by disorder. This mechanism is supported by the temperature dependence of conductance traces, recorded vs  $E_F$ . At few K,  $G$  curves are rather smooth and monotonic, whereas at lower  $T$  fluctuations and resonances show up and regions with positive and negative temperature gradient appear. In the one-electron picture this is explained by thermal averaging which smooths out the interference pattern. At first sight a similar behavior is observed in Fig. 2, yet a closer look discloses important differences.

In order to show temperature dependence of conductance resonances in more detail,  $\Delta G$  values have been calculated by subtracting a smooth curve measured for  $T = 1.75$  K from all other data, collected at lower temperatures. Results are summarized in Fig. 3.  $\Delta G$  reveals five regular oscillations which are smoothed out when temperature increases, however, quite distinct thermal averaging scenarios are found, according to the  $\Delta G$  sign. Conductance antiresonances ( $\Delta G < 0$ ), with positive temperature dependence, are practically unchanged up to  $T \approx 0.5$  K and then start to disappear. At the same time, resonances ( $\Delta G > 0$ ) show stronger, approximately  $T^{-3/2}$ , low-temperature dependence, as demonstrated in Fig. 3(b). Furthermore, up to 20 smaller, quasiperiodic, conductance peaks are superimposed on wider oscillations up to  $G \simeq 2G_0$ . This was not reported in earlier mesoscopic studies of disordered QPCs. The overall picture is therefore more complicated than the one provided by interference of electron waves and suggests a role of the  $e$ - $e$  correlations.

Conductance data presented in Figs. 2 and 3 demonstrate striking similarities with  $G(V_g)$  curves obtained for long ( $\sim 0.8$   $\mu\text{m}$ ) GaAs quantum point contact, with centrally embedded open quantum dot.<sup>8,9</sup> For such a specially designed device, conductance oscillations with reduced height (from  $0.5G_0$  to  $0.8G_0$ , depending on the dot size) were observed in place of a flat plateau. They were interpreted as Fabry-Perot-like resonances, placed above the threshold of each quantized channel. The amplitude of resonances must be reduced, because potential barriers at the entrance and at the exit to the dot will never be exactly the same.<sup>9</sup> Additionally, the Coulomb charging effects in an open dot manifested

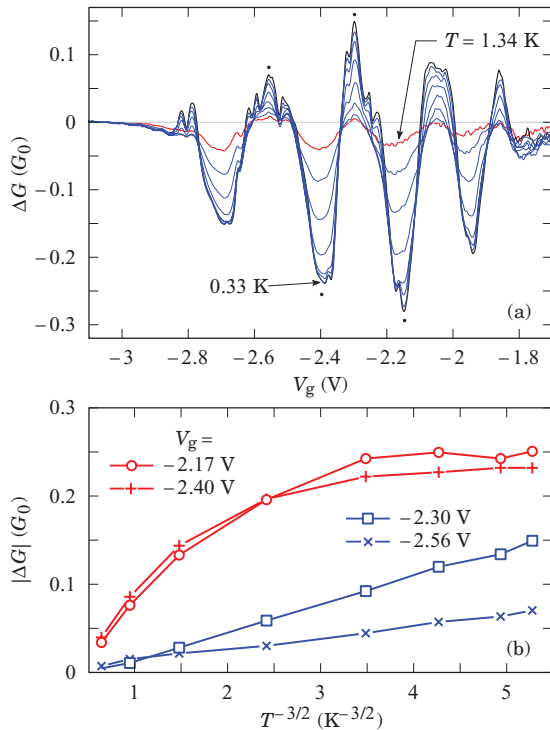


FIG. 3. (Color online) (a) Oscillating part of the zero-bias conductance, defined as  $\Delta G = G(T) - G(T = 1.745 \text{ K})$  as a function of temperature  $T$ , vs gate voltage  $V_g$ . Black line corresponds to  $T = 0.33 \text{ K}$ , red (or gray) line corresponds to  $T = 1.34 \text{ K}$ , all intermediate temperatures are the same as in Fig. 2. (b) The absolute values of  $\Delta G$  as a function of temperature plotted vs  $T^{-3/2}$ . Data marked with blue (dark gray) symbols and lines have been obtained for two maxima of  $\Delta G$ , data marked with red (gray) symbols and lines, for two strongest minima. Corresponding gate voltages are indicated with small dots in (a).

itself as smaller and narrower periodic peaks overlaying upon wider antiresonances. The amplitude of Coulomb peaks increased monotonically down to  $T = 0.05 \text{ K}$ . Clearly, similar features are observed in Fig. 3. Therefore, narrow resonances with  $T^{-3/2}$  temperature dependence may be related to the quantization of charge which gradually fills a shallow potential well when gate voltage increases. Recently, residual charge quantization has been directly observed in a GaAs open quantum dot by capacitance measurements.<sup>10</sup>

Self-consistent calculations suggest that quasilocalized states exist also in a large class of smoothly varying constrictions patterned *without* the intentional central widening. When interactions at wider regions of QPCs are taken into account, the narrowest middle part may be spontaneously charged and form an open dot.<sup>11</sup> This effect is very length dependent—for very short constrictions bound states are not created, whereas for longer devices a chain of charge droplets is predicted to occur.<sup>12</sup> If the device is sufficiently long ( $L > 100 \text{ nm}$ , for GaAs) quasilocalized states may develop also for higher densities, when more than one channel is occupied.<sup>13</sup>

Nevertheless, the physical mechanism of electron localization remains unclear and its influence on conductance measurements is highly debated. Recently, it has been proposed<sup>14</sup> that longitudinal resonant levels are formed within the constriction

due to momentum mismatch and interference effects. In contrast, previous literature suggests<sup>15</sup> that the creation of quasibound states is caused by Friedel oscillations of electron density which emerge at two opposite sides of the QPC and form potential barriers which surround the central part of the device. A barrier for the open channel arises from the interaction with electrons from all closed channels, which are reflected at side boundaries.

Moreover, if Friedel oscillations (FOs) are responsible for barrier formation, the energy averaging must lead to an overall increase in conductance with increased temperature, since then barriers are smoothed. This scenario has recently been supported by numerical simulations and observed experimentally<sup>16</sup> for a clean GaAs quantum wire at  $G > 2G_0$ . A similar effect is also visible in Fig. 2; conductance resonances are smoothed with temperature but their averaged value increases with  $T$ , especially for  $G \gtrsim 1.5G_0$ . We expect that the influence of FOs on transport properties will be larger in CdTe than GaAs, however, such temperature dependence may be also caused by a weak localization effect from the wider regions of our sample.

If weakly bound states are formed, calculations show that the exchange interaction creates a spin-imbalance below the first conduction plateau.<sup>12</sup> This prediction is supported by a large number of experiments carried out for GaAs QPCs at high magnetic fields.<sup>17</sup> Figure 4 shows the effect of an in-plane magnetic field on our device. The number of observed conductance maxima approximately doubles (up to  $B_{\parallel} \approx 3 \text{ T}$ ) evidencing the occurrence of Zeeman effect in each of transmitted channels. The spin splittings of the first two resonances (denoted A and B) are more clearly visible in Fig. 4(b), where the color map of conductance oscillations is shown. A large W-shaped pattern indicates that the energy of spin-down level of the lowest mode A crosses (at  $V_g \approx -1.9 \text{ V}$ ) the energy of spin-up level of the higher channel B. In other words, already at  $B_{\parallel} \approx 7 \text{ T}$  the Zeemann energy becomes comparable to the interlevel spacing  $\epsilon_{1D}$  at  $B = 0$ . It is evident, however, that weaker resonances, presumably related to the charging of quasibound state, behave differently in response to  $B_{\parallel}$ .

For example, a magnetic field that is sufficient to separate the spins of the open 1D channel, does not change the number of weaker conductance resonances ( $\alpha, \beta, \gamma$ ) which are observed for  $G < 0.6G_0$ . In particular, the location of  $\alpha$  and  $\beta$  peaks does not change with field, at the same time resonance  $\gamma$  becomes stronger and moves toward higher energies, however with a smaller slope as compared to channels A and B. The same key feature, i.e., *the absence of spin splitting*, was observed also in a quasiballistic GaAs quantum wire for additional conductance resonances located in the vicinity of a so-called “0.7 anomaly.”<sup>18</sup> We thus find a magnetized regime below the first conduction resonance, which is consistent with GaAs data and with a picture of spin-polarized charge droplets formed within the QPC.<sup>13</sup> On the other hand, for  $G < G_0$  the spin degeneracy of transport channels may be spontaneously lifted without the appearance of localized states<sup>19,20</sup> so further studies are required.

An additional argument for the natural formation of an open dot in our device is provided by the conductance data measured for large source-drain voltages ( $V_{SD} > \epsilon_{1D}$ ).

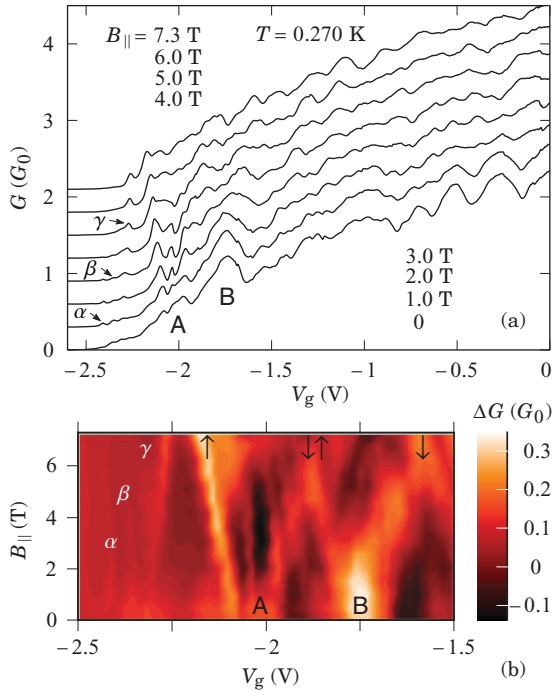


FIG. 4. (Color online) (a)  $G(V_g)$  for  $T = 0.27$  K at various *in-plane* magnetic fields  $B_{\parallel}$ , from 0 (bottom) to 7.3 T (top), collected at different cooldown cycle than data shown in Fig. 2. For clarity curves are shifted vertically by offset of  $0.3 G_0$ . (b) Conductance  $\Delta G$  oscillations as a function of  $V_g$  and  $B_{\parallel}$ , data are obtained from  $G(V_g)$  curves by subtracting a smooth background from each. Labels A and B mark up first two conductance resonances for  $V_g > -2.25$  V, which are split in magnetic field to spin-up and spin-down components (also indicated, negative Landé factor is assumed). Labels  $\alpha$ ,  $\beta$ , and  $\gamma$  denote weaker resonances for  $V_g < -2.25$  V, which are *not split*.

Calculations suggest<sup>21</sup> that if a weakly bound state is present in the constriction, its local density of states follows Fermi energy when gate voltage is changed. As a result, when electrons travel only in one direction (at finite biases), the pinning of the resonant level leads to the appearance of a plateaulike feature at  $G \approx 0.25G_0$  on  $G(V_g)$  curves.<sup>22</sup> Such “0.25 anomaly” was measured for rather long ( $L = 0.4\text{--}1.0 \mu\text{m}$ ) GaAs quantum wires,<sup>18,23,24</sup> where the weakly bound states were present or were probably induced by a strong bias.<sup>3,22</sup> A similar feature is observed also in our shorter device, as it follows from Fig. 5, where  $G(V_g)$  data are presented vs true source-drain voltage  $V_{SD}$  applied to the quantum constriction only.

The displayed values of  $V_{SD}$  have been obtained from the differential conductance data  $G(V_{SD}^*, V_g)$  by a numerical integration procedure and additionally corrected (for  $V_{SD}^* < 1$  mV) due to the nonlinear character of electrical contacts (see above). The formation of a weak shoulder at  $G \approx 0.25G_0$  with increasing source-drain voltage is marked with the horizontal dashed line. The appearance of 0.25 anomaly is more clearly visible at the transconductance  $\partial G/\partial V_g$  curves, displayed in the same figure. Below, in Fig. 5(b) the color map of transconductance is shown for the full ranges of  $V_{SD}$  and  $V_g$  voltages. Data are more complex than typical source-drain spectroscopy patterns obtained for ballistic GaAs QPC, nevertheless the gross features are similar. The conductance

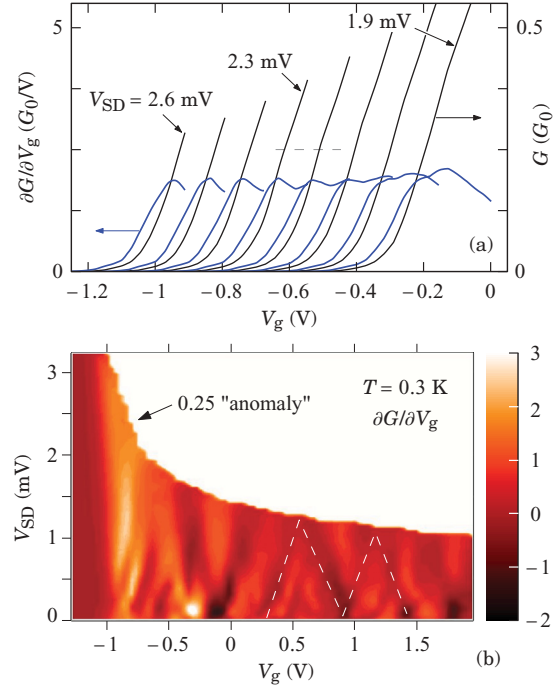


FIG. 5. (Color online) (a)  $G(V_g)$  and  $\partial G/\partial V_g$  for  $T = 0.3$  K at various *source-drain* voltages  $V_{SD}$ , from 2.6 (left) to 1.9 mV (right) with 0.1-mV steps. Curves are successively shifted horizontally by 0.1 V for clarity. (b) Transconductance  $\partial G/\partial V_g$  as a function of  $V_g$  and  $V_{SD}$ . Dashed lines indicate shift of plateaulike regions. Data differ with previous on pinch-off voltage, because they have been measured for a subsequent cooldown cycle.

resonances observed for  $V_{SD} = 0$  merge to a plateaulike features for higher values of dc source-drain polarization. This process is illustrated with white dashed lines for two such plateaus. Presented data suggest that for this particular cooldown cycle, the energy distance between quantized modes  $\epsilon_{1D} = 1.5 \pm 0.5$  meV.

We conclude that many of the observed features of conductance data are shared by longer GaAs wires with centrally embedded open quantum dots. This may seem puzzling since the geometrical aspect ratio of our CdTe devices  $W_{\text{liht}}/L < 1$  and the constriction is formed by a smooth *widenings* on both sides of the short narrowest part. Nevertheless, due to the self-consistent nature of confining potential and stronger interactions in CdTe, the true aspect ratio may become  $W/L \gg 1$  when physical width  $W$  is reduced. To describe this possibility quantitatively we have developed a simple model in which we tried to reproduce the shape of studied QPCs. The most important assumptions and results of calculations are summarized in Fig. 6.

The borders of constriction are defined by two Gaussian functions of half width 200 nm. The external confining potential  $V_{\text{conf}}$  is modelled as an even function, which increases from the center of the device to the edge by 0.8 eV. We have used  $V_{\text{conf}} \sim y^4$  rather than  $\sim y^2$  since the experimental values of  $\epsilon_{1D}$ , inferred from Fig. 5, are better reproduced in the former case. The influence of side-gate voltage on electron confinement has been simulated by changes of constriction width  $W_0$ . For a fixed  $V_{\text{conf}}$  the electron density and effective potential have been calculated self-consistently in Hartree

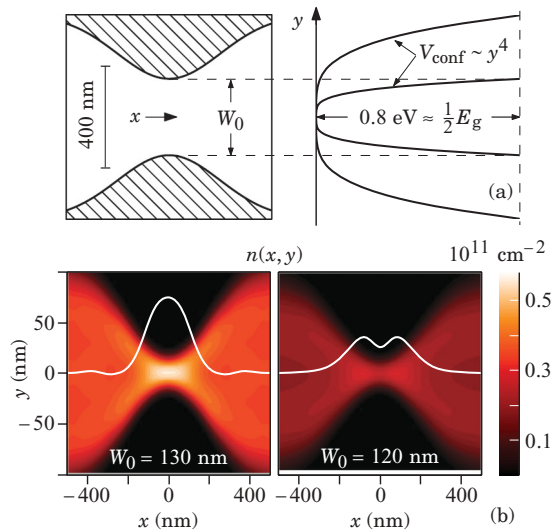


FIG. 6. (Color online) (a) Model of the external confining potential  $V_{\text{conf}}$  for CdTe quantum point contact. Shape of the device in  $(x, y)$  plane is shown on the left. On the right  $V_{\text{conf}}(y) \sim y^4$  is plotted at the constriction of  $W_0$  width (narrower curve) and also far away from it (wider curve),  $E_g$  is the energy gap. (b) Local density of electrons  $n(x, y)$  calculated self-consistently at  $T = 0$  in Hartree approximation for two values of  $W_0$ . Note different scalings on  $x$  and  $y$  axes. White curves represent cross sections of electron density taken along  $y = 0$  line.

approximation along the lines described in Ref. 13, using the Green-function technique. In particular, we have assumed the presence of a positive “mirror charges” located 20 nm above the quantum well plane. To reduce the computational time, we have used a so-called decoupled mode method, which reduces the 2D space to a set of 1D solutions, one for each subband and transverse energy.<sup>25</sup>

Results support our assumption of increased electron density which builds up at the center of the studied device. Interestingly, both possible mechanisms of electron localization seem to operate. For transmitted modes the central pile forms due to the momentum mismatch but also the Friedel oscillations are visible. When constriction width decreases and channel approaches pinchoff, the latter process dominates. As a result, physical aspect ratio increases and the transmission probability may change. However, in order to compare our model with experiment directly a better estimation of  $e$ - $e$  interaction energy is needed. Recent calculations of transport properties for open quantum dots, performed within Hartree-Fock approximation, showed that the nonlocal exchange potential considerably enhances  $n(x, y)$  oscillations and therefore strongly modifies total conductance of the device.<sup>26</sup>

In summary, we have presented low-temperature conductance measurements on short point contact made of a CdTe/CdMgTe quantum well. Data suggest the spontaneous formation of potential barriers at the entrance and at the exit of our device. Recently, the disappearance of quantized plateaus and evidence for the formation of quasibound states in an asymmetrical GaAs QPC have been also reported<sup>27</sup> and attributed to an abrupt rise of confining potential along the channel. Our sample is symmetric and constriction is defined by an adiabatic variation of width, so a momentum mismatch is less severe, yet stronger  $e$ - $e$  interactions in CdTe may induce a natural bound state considerably easier. This makes cadmium telluride a promising host material for studying the interplay between interference and correlation effects in low dimensions.

We acknowledge the support from the Polish Ministry of Science and Higher Education, Project No. N202/103936, and partial support by the European Union within European Regional Development Fund (Innovative Economy Grant No. POIG.01.01.02-00-008/08).

\*adgam@ifpan.edu.pl

<sup>1</sup>B. J. van Wees, L. P. Kouwenhoven, E. M. M. Willems, C. J. P. M. Harmans, J. E. Mooij, H. van Houten, C. W. J. Beenakker, J. G. Williamson, and C. T. Foxon, *Phys. Rev. B* **43**, 12431 (1991).

<sup>2</sup>K.-F. Berggren and M. Pepper, *Philos. Trans. R. Soc. A* **368**, 1141 (2010).

<sup>3</sup>V. A. Sablikov, S. V. Polyakov, and M. Büttiker, *Phys. Rev. B* **61**, 13763 (2000).

<sup>4</sup>P. T. Coleridge, *Phys. Rev. B* **44**, 3793 (1991).

<sup>5</sup>B. A. Piot, J. Kunc, M. Potemski, D. K. Maude, C. Betthausen, A. Vogl, D. Weiss, G. Karczewski, and T. Wojtowicz, *Phys. Rev. B* **82**, 081307 (2010).

<sup>6</sup>S. J. MacLeod, K. Chan, T. P. Martin, A. R. Hamilton, A. See, A. P. Micolich, M. Aagesen, and P. E. Lindelof, *Phys. Rev. B* **80**, 035310 (2009).

<sup>7</sup>J. Wróbel, F. Kuchar, K. Ismail, K. Lee, H. Nickel, and W. Schlapp, *Surf. Sci.* **263**, 261 (1992).

<sup>8</sup>C.-T. Liang, M. Y. Simmons, C. G. Smith, G. H. Kim, D. A. Ritchie, and M. Pepper, *Phys. Rev. Lett.* **81**, 3507 (1998).

<sup>9</sup>O. A. Tkachenko, V. A. Tkachenko, D. G. Baksheev, C.-T. Liang, M. Y. Simmons, C. G. Smith, D. A. Ritchie, G.-H. Kim, and M. Pepper, *J. Phys.: Condens. Matter* **13**, 9515 (2001).

<sup>10</sup>S. Amasha, I. G. Rau, M. Grobis, R. M. Potok, H. Shtrikman, and D. Goldhaber-Gordon, *Phys. Rev. Lett.* **107**, 216804 (2011).

<sup>11</sup>K. Hirose, Y. Meir, and N. S. Wingreen, *Phys. Rev. Lett.* **90**, 026804 (2003).

<sup>12</sup>T. Rejec and Y. Meir, *Nature (London)* **442**, 900 (2006).

<sup>13</sup>S. Ihnatsenka and I. V. Zozoulenko, *Phys. Rev. B* **76**, 045338 (2007).

<sup>14</sup>T. Song and K.-H. Ahn, *Phys. Rev. Lett.* **106**, 057203 (2011).

<sup>15</sup>B. S. Shchamkhalova and V. A. Sablikov, *J. Phys.: Condens. Matter* **19**, 156221 (2007).

<sup>16</sup>V. T. Renard, O. A. Tkachenko, V. A. Tkachenko, T. Ota, N. Kumada, J.-C. Portal, and Y. Hirayama, *Phys. Rev. Lett.* **100**, 186801 (2008).

<sup>17</sup>A. P. Micolich, *J. Phys.: Condens. Matter* **23**, 443201 (2011).

- <sup>18</sup>M. Czapkiewicz, P. Zagrajek, J. Wróbel, G. Grabecki, K. Fronc, T. Dietl, Y. Ohno, S. Matsuzaka, and H. Ohno, *Europhys. Lett.* **82**, 27003 (2008).
- <sup>19</sup>P. Jaksch, I. Yakimenko, and K.-F. Berggren, *Phys. Rev. B* **74**, 235320 (2006).
- <sup>20</sup>A. Lassi, P. Schlagheck, and K. Richter, *Phys. Rev. B* **75**, 045346 (2007).
- <sup>21</sup>S. Ihnatsenka, I. V. Zozoulenko, and M. Willander, *Phys. Rev. B* **75**, 235307 (2007).
- <sup>22</sup>S. Ihnatsenka and I. V. Zozoulenko, *Phys. Rev. B* **79**, 235313 (2009).
- <sup>23</sup>S. M. Cronenwett, H. J. Lynch, D. Goldhaber-Gordon, L. P. Kouwenhoven, C. M. Marcus, K. Hirose, N. S. Wingreen, and V. Umansky, *Phys. Rev. Lett.* **88**, 226805 (2002).
- <sup>24</sup>F. Sfigakis, C. J. B. Ford, M. Pepper, M. Kataoka, D. A. Ritchie, and M. Y. Simmons, *Phys. Rev. Lett.* **100**, 026807 (2008).
- <sup>25</sup>Z. Ren, R. Venugopal, S. Goasguen, S. Datta, and M. S. Lundstrom, *IEEE Trans. Electron Devices* **50**, 1914 (2003).
- <sup>26</sup>S. Ihnatsenka, *Physica E* **44**, 1209 (2012).
- <sup>27</sup>P. M. Wu, P. Li, H. Zhang, and A. M. Chang, *Phys. Rev. B* **85**, 085305 (2012).